Characterization of gasifier condensate as a potential replacement of asphalt binder

Bhaswati Bora & Nikhil Saboo & Praveen Kumar & Sonal K. Thengane
IIT Roorkee, Roorkee, UK, India

ABSTRACT: Biobased materials and byproducts of bio refineries are explored as alternative materials to replace the fossil fuel-based binders. Biomass or biowaste are processed and chemically treated to a compatible form to blend with asphalt binder homogeneously. In this study, gasifier byproduct of pine needle biomass was investigated as a potential replacement of asphalt binder. Replacement up to 20 % was studied and the binders were chemically characterized using FTIR and TGA. Correlations were developed between the chemical indices and the physical properties. For morphological analysis, imaging studies were performed using AFM. It was found that the gasifier bio-condensate has some potential for use as a replacement for asphalt binders. The bio-condensate also showed a rejuvenation effect, as observed from chemical and morphological studies.

1 INTRODUCTION

Life cycle assessment of asphalt binder shows significant CO_2 and GHG emissions. Lignocellulosic biomass and biowaste have been explored as alternative sustainable resources for asphalt binder replacement that can substantially reduce these emissions. Biomass is initially chemically treated to convert into compounds with a similar composition as that of the asphalt binder. The thermochemical conversion process is the most effective method for converting biomass into biobased carbonaceous materials. Past studies have performed pyrolysis and hydrothermal liquefaction on plant-based and waste biomass to obtain bio-oil as a replacement for asphalt binder. Literature survey indicates mixed performance results of bio-asphalt binder (with a replacement up to 40%). Due to the softening of the base binder with the use of higher dosage of bio-oil, polymer modification of the bio-asphalt has also been explored in a few studies (He et al. 2020; Al-Sabaeei et al. 2020).

Biomass condensate obtained from a gasifier facility was used in this study as a partial replacement of asphalt binder. In general, a gasifier facility is used for syngas production from biobased feedstock such as lignocellulosic, bio-waste, or other carbonaceous resources. They are sustainable production systems for producing clean and green alternative forms of energy over fossil fuel-based natural resources. The gasifier operates at high temperatures of 800°C to 1100°C for biomass conversion into sustainable renewable energy in the presence of oxygen. The feedstock is initially pretreated for moisture removal. The gasifier operates through a series of physicochemical processes occurring inside the reactor, such as combustion reaction, pyrolysis, cracking, reforming, oxidation, and reduction producing gas and char as primary products. Other than syngas and char production, higher production temperatures lead to the formation of a byproduct. This condenses on the reactor bed after cooling the gasifier. Gasifier condensate is a combination of heavy metals, oil, fly ash, tar, and low-carbonaceous materials. The condensate is recovered as a mixture of water during the cleaning process of the gasifier. The composition of the gasifier condensate is widely dependent on feedstock source, operating conditions, and gasifier type.

In this study, gasifier condensate of pine needle biomass was investigated as a potential replacement for asphalt binder. The bio-asphalt binders were prepared by replacing the base binder with 5%, 10%, 15%, and 20% bio-condensate (by weight of the base binder). The bio-condensate and the prepared bio-asphalt binder were characterized using Fourier Transform Infrared (FTIR) spectroscopy to identify the chemical composition of the condensate and the bio-asphalt binder. Thermal stability, mass loss, and residue analysis were performed on the prepared bio-asphalt using Thermogravimetric Analyzer (TGA). The aging performance of the bio-asphalt binder was further investigated using physical, rheological, and chemical analysis. Finally, morphological investigations were performed using Atomic Force Microscopy (AFM) to understand the interaction between base binder and bio-condensate at different aging conditions.

2 EXPERIMENTAL STUDIES

2.1 *Bio-asphalt production*

A VG-40 binder, as per IS 73-2013, was used as the base binder in this study. The condensate obtained from the gasification process was heated initially at a controlled temperature of 150°C to remove water. Volatiles and lightweight compounds also get removed with water at this temperature. The recovered condensate had a homogeneously viscous oily tex-

ture. The dewatered bio-condensate was added to the preheated asphalt binder at 135°C. (Zhang et al. 2020). The condensate and the asphalt binder were mechanically mixed with a stirrer rotating at 1500 rpm for 20 mins at 135°C to prepare the bio-asphalt binder. Low blending temperatures were considered for bio-asphalt production to ensure that the inherent properties are not affected by the production temperatures. The homogeneity of the produced bio-asphalt binder was assessed visually.

2.2 *FTIR analysis*

FTIR spectroscopy can be used to evaluate the functional groups and compounds present in any material. The quantification of the compounds present in the asphalt binder is typically performed by calculating the indices of the functional groups and compounds. Carbonyl (C=O) and sulfoxide (S=O) indices are generally used to quantify aging in the asphalt binder (refer to Equations 1 and 2). The samples in this study were tested using the KBr pellet method. Sample solutions were prepared using CS_2 as a solvent and 10 microliters of the sample solution was drop casted on the KBr pellet to test using the FTIR spectroscopy (Bora & Das 2020, 2021). 32 scans were performed per sample to obtain the absorbance spectra. 4 cm^{-1} resolution was used during the experiment.

$$I_{C=0} = \frac{I_{1700}}{I_{REF}} \quad (1)$$

$$I_{S=0} = \frac{I_{1030}}{I_{REF}} \quad (2)$$

2.3 *TGA analysis*

The temperature stability and mass loss of the bio-asphalt binder can be analyzed using a thermogravimetric analyzer. The decomposition kinetics and the degradation behaviors of asphalt binders at higher temperatures were investigated using the TGA. For TGA analysis, around 10 mg of binder sample was tested from 30°C to 800°C under inert conditions at a heating rate of (10°C)/min.

2.4 *AFM analysis*

Images of the base binder and the bio-asphalt binder were captured using the PeakForce Quantitative Nanomechanics (QNM) mode of scanning. Catanaphase, periphase, and paraphase are the three phases of asphalt binder identified using the AFM. Sometimes waxes are identified as a fourth phase and are observed as a bright phase on the AFM images. In this study, AFM imaging was performed on the base binder and bio-asphalt binders to identify the wax content and the phase changes on modification and aging (Das et al. 2016, Yu et al. 2016). A force of 272μN was applied on the cantilever probe having a spring constant 40.41 N/m and a tip radius of 64.56 nm for the QNM mode of scanning.

2.5 *Physical properties*

The softening point (SP) (ASTM D36/D36M-14) and the high-temperature true fail (T/F) temperature (AASHTO 2017) of the binders were evaluated for the unaged binder, short-term aged (STA) binder, and long-term aged (LTA) binder. The short-term aging index (STAI) was calculated using the values of SP and T/F temperatures. Long-term aging index (LTAI) was also determined using SP values. The mathematical definition of the aging index (AI) is presented through Equation (3). Similarly, the AI using FTIR chemical indices ($I_{C=O}$ and $I_{S=O}$) were used to study the susceptibility of the binders to aging.

$$Aging\ index\ (AI) = \frac{Parameter\ value\ after\ aging}{Parameter\ value\ before\ aging} \quad (3)$$

3 ANALYSIS AND RESULTS

The values of SP and the T/ F temperatures are presented in Table 1 and Table 2, respectively. In general, with aging, the SP of all the binders increased. Irrespective of the type of binder, the increase in SP after STA and LTA was found to be approximately 5°C and 18°C, respectively. Addition of bio-condensate led to marginal reduction in the SP. With increase in the dosage of the bio-condensate, the SP values were found to reduce. Interestingly, these results of T/F temperature were not in agreement with the results of SP. At 15% and 20% replacement, the bio-asphalt binder showed significant increase in stiffness after STA. In other words, at higher replacement dosages, the bio-asphalt binder may be more prone to aging. More studies are required to explain the difference in the results of SP and T/F temperature.

Table 1. Softening point (SP) of binders.

	VG-40	5% rep	10% rep	15% rep	20% rep
Unaged (UA)	52.5	51	50.9	50.8	50.8
STA	58.5	59.1	58.4	57.1	55.6
LTA	71.2	70.4	70.2	69.1	69.3

Table 2. High temperature PG and T/F temperature.

		VG-40	5% rep	10% rep	15% rep	20% rep
UA	Fail Temp	82	76	76	76	76
	P/F Temp	76.3	72.4	72.2	72.1	70.7
STA	Fail Temp	82	82	82	118	118
	P/F Temp	80.5	81	80.4	117.9	117

Figure 1 represents the peaks in the fingerprint region of the FTIR spectra of the 5% bio-asphalt binder in different aging conditions. Similar peaks pre-

sent in the bio-oil was observed in the bio-asphalt binder. However, amines, ester, ether, anhydrides, and substituted aromatic compounds were not observed in the asphalt binder. Also, the -OH groups and the compounds formed due to presence of the hydroxyl compounds are absent in the bio-asphalt binder (refer to Figure 1). S=O formation, which typically occurs on aging, is observed at 1060 cm^{-1}. Cyclic compounds such as cyclic alkenes, cyclic amides, and aromatic compounds with C=O groups i.e., amide, lactam, and carboxylic acid are observed to be present in both bio-asphalt binder and bio-oil. On short-term aging no peak degradation is observed in peaks between 1560 cm^{-1} and 1760 cm^{-1}. However, on long-term aging the peaks due to the cyclic compounds, amides, acids, unsaturated ketones decompose. -OH compounds also decompose on aging observed form the peak at 3440 cm^{-1}. On the contrary, no degradation is observed in the alkene peaks at 1647 cm^{-1} and 1654 cm^{-1} on aging.

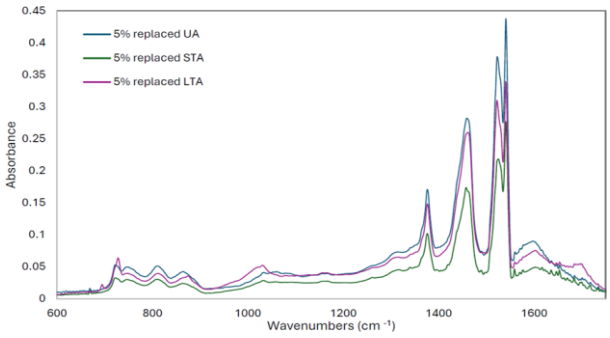

Figure 1. 5% bio-asphalt binder spectra on aging.

Figure 2 shows the C=O indices of the bio-asphalt binders and VG-40. C=O generally increases on aging, as observed for all the binders. The C=O values of 5% bio-asphalt binder are higher than VG-40 and decrease with the increase in the bio-condensate percentage. The decrease in C=O values is the rejuvenation effect of the bio-asphalt binder. The unsaturated ketones, amides, and acids containing C=O decompose on biomodification using gasifier bio-condensate, leading to occurrence of such effect. Similar results were observed for long-term aged S=O, as presented in Figure 3. The S=O decomposes for the higher bio-condensate percent, i.e., the bio-condensate reduces S=O formation after STA and LTA. However, an increase in S=O was observed with the percent increase in bio-condensate.

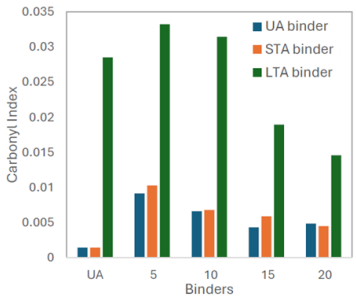

Figure 2. C=O index of bio-asphalt binder.

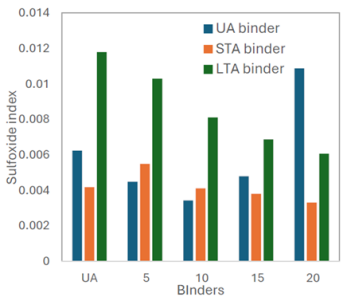

Figure 3. S=O index of bio-asphalt binder.

3.1 *Aging Index*

The chemical indices obtained using FTIR were correlated with the binder's physical properties. Good correlation is observed between the SP and C=O index after STA. Similarly, good correlation between T/F temp and C=O index after STA was seen. Good correlation is observed between SI and SP for STA samples, but a poor correlation was obtained between the SI and SP after LTA. This is due to S=O decomposition reactions at higher temperatures. Additionally, poor correlation between the SI and the T/F temp is observed after STA. The R^2 value for all the correlation analysis is presented in Table 3. Inconsistencies in correlations under different aging conditions and between different material properties require further investigations.

Table 3. Correlation values R^2 of the chemical indices with the physical properties.

	STAI	LTAI
CI vs SP	0.94	0.80
SI vs SP	0.98	0.83
CI vs PG	0.92	-
SI vs PG	0.80	-

3.2 *TGA analysis*

Figure 4 represents the TGA decomposition graph of the base binder and the bio-asphalt binders. A two-step decomposition graph was observed for the bio-asphalt binder whereas, a one-step decomposition graph was seen for the base asphalt binder. The mass loss observed for all the asphalt binders follows a similar reaction path and is found to vary from 85% to 88%. The first stage decomposition was observed at 116°C for the 5% bio-binder, which decreases to 110°C for the 20% bio-binder. The decomposition for the base asphalt binder was found to be approximately 239°C for the base asphalt binder. The second stage decomposition temperature increased on asphalt replacement to 291°C and decreased with the bio-condensate replacement percentage to 275°C. Similar results were observed with the final decomposition temperatures at both the decomposition stages for all the binders.

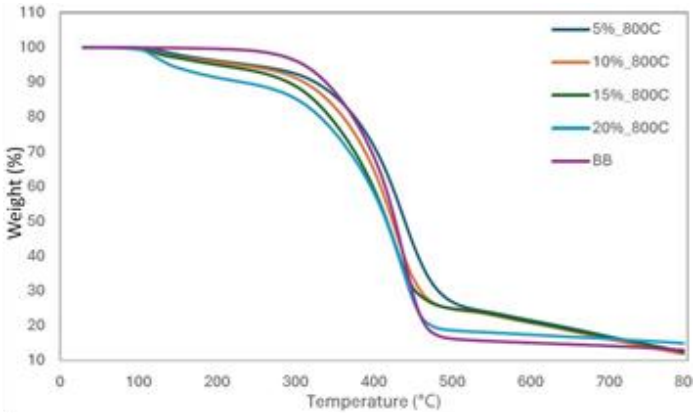

Figure 4. Thermogravimetry (TGA) graph

3.3 *AFM analysis*

The AFM images of the base asphalt binder showed three distinct phases on the binder surface (refer Figure 5). The three phases observed in asphalt binder, i.e., catena phase (bee structures), periphase, and paraphase can be identified distinctly on the base asphalt binder surface. Bee structure agglomeration can be observed for the LTA binders due to the increase in the asphaltene structures. In the case of the bio-asphalt binders only two phases can be identified. Also, the bee structures appear to dissolve in the periphase. This is due to the increase in the lighter components in the bio-asphalt binder due to the presence of bio-condensate. Also, asphaltene deagglomeration occurs in the bio-asphalt binder as the periphase and the catanaphase disintegrate due to the rejuvenation effect of the bio-asphalt binder. The restoration effect is also indicated by the C=O indices, which decrease with the increase in replacement percentage. Morphologically, the base binder structure is affected due to the replacement with the gasifier bio-condensate. Further investigations are required to assess the effect of the morphological changes on the binder performance.

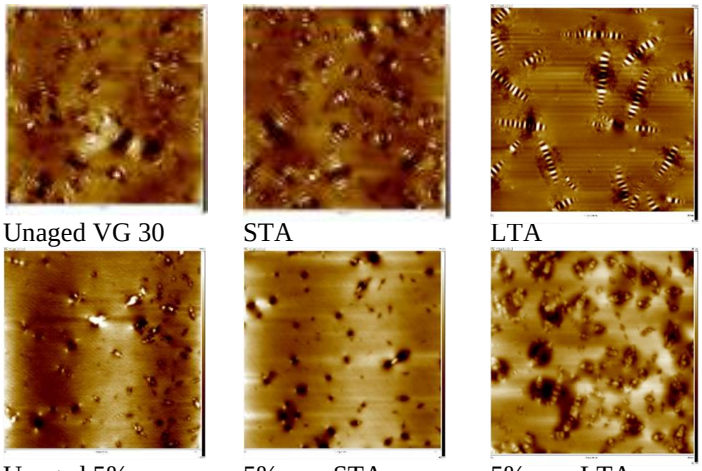

Figure 5. Morphological images of the binders through AFM.

4 CONCLUSIONS

This study investigated the characterization of bio-condensate replaced asphalt binder chemically using FTIR and TGA. Physical properties were measured and correlated with the chemical indicators. Also imaging studies were performed to investigate the morphological changes due to the addition of bio-condensate. Following conclusions were drawn:

- The SP reduced by 2°C on replacement up to 20% using gasifier bio-condensate. Similarly, the high temperature PG reduced by one grade up to 20% replacement.
- The CI and SI aging indices from FTIR showed a good correlation with the aging indices of the physical properties.
- Although moisture decomposition is observed in the TGA graphs from the bio-condensate replaced binders, the thermal stability of all the bio-condensate replaced binders increased.
- Removal of moisture occurs from the bio-asphalt binders on aging. This was observed from the -OH values and from TGA graphs. This is due to higher -OH compounds in the bio-condensate.
- The bio-condensate also has a rejuvenation effect, decreasing the C=O index. This was observed from the bee structure deagglomeration images from AFM morphological studies.

This study establishes the use of condensate from gasifier as a potential biobased material for asphalt binder replacement. The characterization studies on bio-condensate replaced binders up to 20% shows a potential for replacement of asphalt binder with the pine needle gasifier condensate. Further investigations on bio-asphalt binder rheology and performance evaluation of the bio-condensate replaced asphalt mixtures are required to explain the potential of gasifier condensate as a sustainable replacement of asphalt binders in the future. In addition, the potential for the use of gasifier condensate as a recycling agent for RAP binders can be further explored.

ACKNOWLEDGMENT

The authors would like to thank Ministry of Roads Transport and Highways (MoRT&H), India, for supporting the project (RS/IITRoorkee/2023-24/S&R (P&B)-03).

REFERENCES

Al-Sabaeei A. M., et al. 2020. A systematic review of bio-asphalt for flexible pavement applications: Coherent taxonomy, motivations, challenges and future directions, J. Clean. Prod., 249, 119357

ASTM D36/D36M-14. (2014). *Standard test method for softening point of bitumen.* ASTM International.

AASHTO M 320. 2017. *Standard Specification for Performance-Graded Asphalt Binder*. Washington, DC.

Bora B., & Das A. 2020. Estimation of binder quantity in binary mixture of asphalt binders. *Transp. Res. Proc.*, 48, 3756–3763.

Bora B., & Das A. 2021. Blending of RAPM samples with virgin binder: A study using FTIR spectroscopy. *IOP Conf. Ser.: Mat. Sci. and Engg.*, Malaysia, 1075, 012016.

He L. et al. 2023. Biomass valorization toward sustainable asphalt pavements: progress and prospects, *J. Waste Manag.*, 165, 159–178.

IS:73. 2013. *Paving bitumen - specification. New Delhi, India, Bur. Indian stand*. Indian standards institution, (1–4).

Rosyidi S.A.P et al. 2022. Physical, chemical and thermal properties of palm oil boiler ash/rediset-modified asphalt binder, *Sustain.*, 14(5), 3016.

Das P. K., Baaj H., Tighe S., & Kringos N. 2016. Atomic force microscopy to investigate asphalt binders: A state-of-the-art review. *Road Mater. Pavement*, 17(3), 693–718.

Yu X., Burnham N. A., & Tao M. 2015. Surface microstructure of bitumen characterized by atomic force microscopy, *Adv. Coll. Int. Sci.*, 218, 17–33.

Zhang X. et al. 2020. Preparation of bio-oil and its application in asphalt modification and rejuvenation: A review of the properties, practical application and life cycle assessment, *Constr. Build. Mater.*, 262, 120528.